 CMES, vol.2, no.2, pp.213-226, 2001

An Advanced Time-Discontinuous Galerkin Finite Element Method for Structural Dynamics

Chyou-Chi Chien, Tong-Yue Wu[1]

Abstract: This study presents a novel computational method for implementing the time finite element formulation for the equations of linear structural dynamics. The proposed method adopts the time-discontinuous Galerkin method, in which both the displacement and velocity variables are represented independently by second-order interpolation functions in the time domain. The solution algorithm derived utilizes a predictor/multi-corrector technique that can effectively obtain the solutions for the resulting system of coupled equations. The numerical implementation of the time-discontinuous Galerkin finite element method is verified through several benchmark problems. Numerical results are compared with exact and accepted solutions from previous literature. Since a fifth-order accurate algorithm ensues by using quadratic interpolations for displacement and velocity, numerical results significantly improve in stability and accuracy for structural dynamics problems.

keyword: Time-discontinuous Galerkin method, finite element method, stability, accuracy, structural dynamics.

1 Introduction

Most finite element procedures for structural dynamic or elastodynamic problems are based on semi-discretizations: finite elements are used in space to reduce a system of second-order ordinary differential equations in time which are in turn discretized by traditional finite difference methods for ordinary differential equations. These governing equations for discrete models are known as the semi-discrete equations of structural dynamics or elastodynamics. Many finite difference algorithms for direct time integration methods of structural dynamics have been developed in recent decades [Newmark (1959); Wilson, Farhoomand and Bathe (1973); Houbolt (1950); Hilber, Hughes and Taylor (1977)]. Among these, second-order accurate methods, such as the Newmark-β method (1959), the Wilson-θ method (1973), the Houbolt method (1950), and the HHT-α method (1977), are most frequently used in practice. As widely assumed, the finite element method is superior to finite difference method. If finite elements have advantages in space, they should also have advantages in time [Hughes and Hulbert (1988)]. Thus, many researchers have attempted to use finite elements in the time domain [Argyris and Scharp (1969); Fried (1969); Oden (1969); Zienkiewicz and Taylor (1991)]. Kinematic and mixed formulation for dynamics were derived from a general form and multibody simulations were carried out using finite elements in the time domain [Mello, Borri and Atluri (1990); Borri, Mello and Atluri (1990)]. Further, a general framework for interpreting time finite element formulations was proposed by Borri and Bottasso (1993). The goal of their study was to provide a unified view, where different methods emanate from the same general statement of the problem of motion expressed by Hamilton's law of varying action. Within this framework, the bi-discontinuous form and the discontinuous Galerkin form for integration algorithms were derived respectively, according to different boundary terms.

Another finite element approach in the time domain is based on a time-discontinuous Galerkin (TDG) method. This method allows the unknown fields to be discontinuous at the discrete time levels. The TDG method has been successfully applied to first-order hyperbolic problems [Johnson, Nävert and Pitkaranta (1984)] (fluid mechanics) and parabolic problems [Johnson (1987); Thomée (1984)] (transient heat conduction). Hughes and Hulbert (1988) first applied this novel approach to the area of structural dynamics, demonstrating that the TDG method possesses considerable potential not present in the traditional semi-discrete methods. In particular, it leads to A-stable, higher-order accurate solution algorithms to solve ordinary differential equations and, in doing so, achieves the asymptotic annihilation of the spurious high

[1] Department of Civil Engineering, Chung-Yuan University, Chung-Li, 32023, Taiwan. e-mail: chyouchi@cycu.edu.tw

frequency response [Hulbert and Hughes (1990); Hulbert (1992)]. Li and Wiberg (1996, 1998) recently applied the TDG method to two-dimensional structural dynamic problems. In particular, that investigation dealt with the specific TDG method that uses piecewise linear interpolations for both displacements and velocities, i.e., P1-P1 two-field formulation element [Hulbert (1992)]. For this type of element, that same investigation also applied an adaptive procedure to update the time steps and the spatial meshes, making the solutions reliable. According to above results, the TDG method using P1-P1 element is of third-order accuracy in time [Hulbert (1992)].

In the light of above developments, this study presents a specific time-discontinuous Galerkin method that independently uses the piecewise quadratic-in-time interpolation functions for both the displacements and velocities, i.e., the P2-P2 two-field formulation element. This type of element has very little numerical dissipation or amplitude decay in the low-frequency regime. The frequency error or period elongation when using the P2-P2 algorithm is virtually negligible in the low-frequency regime, reflecting its fifth-order accuracy [Hulbert (1994)]. The P2-P2 element appears to have an advantage over the P1-P1 element with respect to stability and accuracy. Although a related study has analyzed contact/impact problems with a displacement TDG finite element formulation (i.e., the P2 single-field element) [Karaoğlan and Noor (1997)], some rather troublesome least-square stabilizer operators must be added to the governing equations to enhance stability by smoothing out the high frequency modes. To our knowledge, no work has numerically implemented the TDG finite element method when utilizing the P2-P2 element for structural dynamic analysis. Hence, this study focuses mainly on how to implement an advanced time-discontinuous Galerkin finite element method using the P2-P2 element. A predictor/multi-corrector iteration technique for the solution of algorithms is adopted to make the computation efficient. Finally, numerical results from using the P2-P2 and P1-P1 algorithms to solve structural dynamic problems are compared.

2 Time-discontinuous Galerkin Finite Element Method Formulation

The equation of motion for a linear multi-DOF structural system subjected to external force is the second-order differential equation:

$$\mathbf{M}\ddot{\mathbf{u}} + \mathbf{C}\dot{\mathbf{u}} + \mathbf{K}\mathbf{u} = \mathbf{F} \tag{1}$$

where $\mathbf{M}$ denotes the mass matrix, $\mathbf{C}$ represents the viscous damping matrix, $\mathbf{K}$ is the stiffness matrix, $\mathbf{F}$ denotes the vector of applied forces, and $\ddot{\mathbf{u}}$, $\dot{\mathbf{u}}$ and $\mathbf{u}$ represent the acceleration, velocity and displacement vectors, respectively. The initial displacement $\mathbf{u}(0)$ and initial velocity $\dot{\mathbf{u}}(0)$ at time zero must be specified to define the problem completely. This section employs a specific time-discontinuous Galerkin method which uses piecewise quadratic interpolations for both the displacement and velocity. This is the TDG element named as the P2-P2 two-field formulation [Hulbert (1992, 1994)]. The formulations of the TDG method are briefly reviewed as follows.

Let $0 = t_1 < t_2 < \ldots < t_n < t_{n+1} < \ldots < t_{N+1} = T$ be a partition of the time domain $I = (0,T)$ with corresponding time steps $\Delta t_n = t_{n+1} - t_n$ and $I_n = (t_n, t_{n+1})$. Making the following equation represents the specific choice of the time finite element space:

$$\mathbf{V}^h = \left\{ \mathbf{w}^h \in \bigcup_{n=1}^{N} \left(P^2(I_n) \right)^{n_{eq}} \right\} \tag{2}$$

where P^2 denotes the second-order polynomial, and each member of $\mathbf{V}^h$ represents a vector consisting of n_{eq} quadratic functions on each time step I_n. All trial displacements and velocities and their corresponding weighting functions are chosen from the space $\mathbf{V}^h$. Notably, the functions in $\mathbf{V}^h$ may be discontinuous at the discrete time levels t_n, as seen in Fig. 1. This can be accounted for by the following notations:

$$\mathbf{w}_n^+ = \lim_{\varepsilon \to 0^+} \mathbf{w}(t_n + \varepsilon) \tag{3a}$$

$$\mathbf{w}_n^- = \lim_{\varepsilon \to 0^-} \mathbf{w}(t_n + \varepsilon) \tag{3b}$$

$$[\mathbf{w}_n] = \mathbf{w}_n^+ - \mathbf{w}_n^- \tag{3c}$$

where $[\mathbf{w}_n]$ represents the jump of $\mathbf{w}_n$ at t_n, and the inner product on I_n is denoted by:

$$(\mathbf{w}, \mathbf{u})_{I_n} = \int_{I_n} \mathbf{w} \cdot \mathbf{u} \, dt \tag{4}$$

The time-discontinuous Galerkin finite element method can now be formulated as follows:

Find $\mathbf{U}^h = \{\mathbf{u}^h, \mathbf{v}^h\} \in \mathbf{V}^h \times \mathbf{V}^h$ such that for all $\mathbf{W}^h = \{\mathbf{w}_1^h, \mathbf{w}_2^h\} \in \mathbf{V}^h \times \mathbf{V}^h$

$$\mathbf{B}_{DG}\left(\mathbf{W}^h, \mathbf{U}^h\right)_n = \mathbf{L}_{DG}\left(\mathbf{W}^h\right)_{n,} \qquad n = 1, 2, ..., N \tag{5}$$

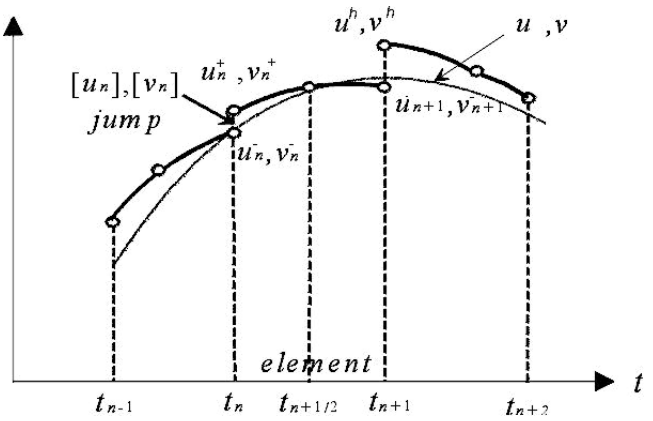

Figure 1 : Illustration of time-discontinuous functions

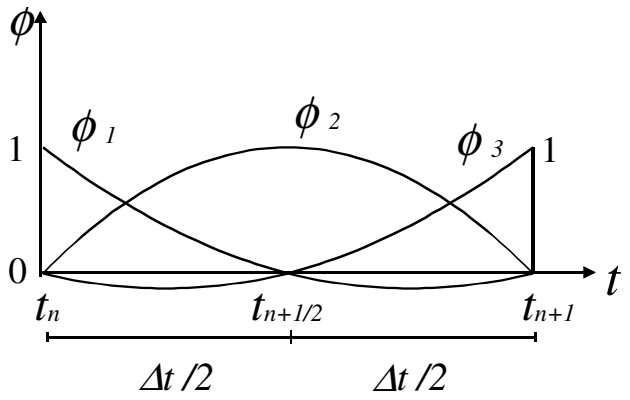

Figure 2 : Time-discontinuous interpolation functions

where

$$\mathbf{B}_{DG}\left(\mathbf{W}^h,\mathbf{U}^h\right)_n=\left(\mathbf{w}_2^h,\mathbf{L}_1\mathbf{U}^h\right)_{In}+\left(\mathbf{w}_1^h,\mathbf{K}\mathbf{L}_2\mathbf{U}^h\right)_{In}+\mathbf{w}_2^h\left(\mathbf{t}_n^+\right)\cdot\mathbf{M}\mathbf{v}^h\left(\mathbf{t}_n^+\right)+\mathbf{w}_1^h\left(\mathbf{t}_n^+\right)\cdot\mathbf{K}\mathbf{u}^h\left(\mathbf{t}_n^+\right)$$
$$n=1,2,.....N \tag{6}$$

$$\mathbf{L}_{DG}\left(\mathbf{W}^h\right)_n=\left(\mathbf{w}_2^h,\mathbf{F}\right)_{In}+\mathbf{w}_2^h\left(\mathbf{t}_n^+\right)\cdot\mathbf{M}\mathbf{v}^h\left(\mathbf{t}_n^-\right)+\mathbf{w}_1^h\left(\mathbf{t}_n^+\right)\cdot\mathbf{K}\mathbf{u}^h\left(\mathbf{t}_n^-\right)$$
$$n=2,\cdots N \tag{7}$$

$$\mathbf{L}_{DG}\left(\mathbf{W}^h\right)_1=\left(\mathbf{w}_2^h,\mathbf{F}\right)_{I_1}+\mathbf{w}_2^h\left(0^+\right)\cdot\mathbf{M}\mathbf{v}_0+\mathbf{w}_1^h\left(0^+\right)\cdot\mathbf{K}\mathbf{u}_0$$
$$n=1 \tag{8}$$

and

$$\mathbf{L}_1\mathbf{U}^h=\mathbf{M}\dot{\mathbf{v}}^h+\mathbf{C}\mathbf{v}^h+\mathbf{K}\mathbf{u}^h \tag{9}$$

$$\mathbf{L}_2\mathbf{U}^h=\dot{\mathbf{u}}^h-\mathbf{v}^h \tag{10}$$

Hulbert (1994) indicated that this time-discontinuous Galerkin method using P2-P2 formulation is unconditionally stable and of fifth-order accuracy.

3 Numerical Implementation and Solution Algorithm

This section presents the equivalent matrix form of Eq. 5 and an iterative solution algorithm to solve the resulting system of equations. While considering a typical time step $I_n=(t_n,t_{n+1})$, let $\mathbf{u}_1$ and $\mathbf{v}_1$ denote the nodal displacements and velocities at t_n^+, respectively, $\mathbf{u}_2$ and $\mathbf{v}_2$ the nodal displacements and velocities at $t_{n+1/2}$, respectively, and $\mathbf{u}_3$ and $\mathbf{v}_3$ the nodal displacements and velocities at t_{n+1}^-, respectively. Let $\mathbf{u}_1^-$ and $\mathbf{v}_1^-$ represent the nodal displacements and velocities at t_n^-, respectively, which are determined from either the previous step's calculations or, if $n=1$, from the initial data. Also, let $\boldsymbol{f}_1$, $\boldsymbol{f}_2$, and $\boldsymbol{f}_3$ denote the nodal forces at t_n, $t_{n+1/2}$ and t_{n+1}, respectively. Thus, the displacements, velocities, and forces at an arbitrary point x and time $I_n\in(t_n,\,t_{n+1})$ can be expressed as

$$\mathbf{u}^h(t)=\phi_1\mathbf{u}_1+\phi_2\mathbf{u}_2+\phi_3\mathbf{u}_3 \tag{11a}$$
$$\mathbf{v}^h(t)=\phi_1\mathbf{v}_1+\phi_2\mathbf{v}_2+\phi_3\mathbf{v}_3 \tag{11b}$$
$$\mathbf{f}^h(t)=\phi_1\mathbf{f}_1+\phi_2\mathbf{f}_2+\phi_3\mathbf{f}_3 \tag{11c}$$

where$\phi_1=2\left(\frac{t-t_n}{\Delta t}\right)^2-3\left(\frac{t-t_n}{\Delta t}\right)+1$, $\phi_2=-4\left(\frac{t-t_n}{\Delta t}\right)^2+4\left(\frac{t-t_n}{\Delta t}\right)$ and $\phi_3=2\left(\frac{t-t_n}{\Delta t}\right)^2-\left(\frac{t-t_n}{\Delta t}\right)$ and Δt = t_{n+1}-t_n, as seen in Fig. 2.

Substituting Eq. 11 and their corresponding weighting functions into Eq. 5, and performing the integration explicitly, yields the following matrix equation:

$$\begin{bmatrix}
\frac{1}{2}\mathbf{K} & \frac{2}{3}\mathbf{K} & -\frac{1}{6}\mathbf{K} & -\frac{2}{15}\Delta t\mathbf{K}\\
-\frac{2}{3}\mathbf{K} & \mathbf{0} & \frac{2}{3}\mathbf{K} & -\frac{1}{15}\Delta t\mathbf{K}\\
\frac{1}{6}\mathbf{K} & -\frac{2}{3}\mathbf{K} & \frac{1}{2}\mathbf{K} & \frac{1}{30}\Delta t\mathbf{K}\\
\frac{2}{15}\Delta t\mathbf{K} & \frac{1}{15}\Delta t\mathbf{K} & -\frac{1}{30}\Delta t\mathbf{K} & \frac{1}{2}\mathbf{M}+\frac{2}{15}\Delta t\mathbf{C}\\
\frac{1}{15}\Delta t\mathbf{K} & \frac{8}{15}\Delta t\mathbf{K} & \frac{1}{15}\Delta t\mathbf{K} & -\frac{2}{3}\mathbf{M}+\frac{1}{15}\Delta t\mathbf{C}\\
-\frac{1}{30}\Delta t\mathbf{K} & \frac{1}{15}\Delta t\mathbf{K} & \frac{2}{15}\Delta t\mathbf{K} & \frac{1}{6}\mathbf{M}-\frac{1}{30}\Delta t\mathbf{C}
\end{bmatrix}$$

$$\begin{bmatrix} -\frac{1}{15}\Delta t\mathbf{K} & \frac{1}{30}\Delta t\mathbf{K} \\ -\frac{8}{15}\Delta t\mathbf{K} & -\frac{1}{15}\Delta t\mathbf{K} \\ -\frac{1}{15}\Delta t\mathbf{K} & -\frac{2}{15}\Delta t\mathbf{K} \\ \frac{2}{3}\mathbf{M}+\frac{1}{15}\Delta t\mathbf{C} & -\frac{1}{6}\mathbf{M}-\frac{1}{30}\Delta t\mathbf{C} \\ \frac{8}{15}\Delta t\mathbf{C} & \frac{2}{3}\mathbf{M}+\frac{1}{15}\Delta t\mathbf{C} \\ -\frac{2}{3}\mathbf{M}+\frac{1}{15}\Delta t\mathbf{C} & \frac{1}{2}\mathbf{M}+\frac{2}{15}\Delta t\mathbf{C} \end{bmatrix} \begin{Bmatrix} \mathbf{u}_1 \\ \mathbf{u}_2 \\ \mathbf{u}_3 \\ \mathbf{v}_1 \\ \mathbf{v}_2 \\ \mathbf{v}_3 \end{Bmatrix}$$
$$= \begin{Bmatrix} \mathbf{K}\mathbf{u}_1^- \\ \mathbf{0} \\ \mathbf{0} \\ \frac{\Delta t}{30}(4\mathbf{f}_1+2\mathbf{f}_2-\mathbf{f}_3)+\mathbf{M}\mathbf{v}_1^- \\ \frac{\Delta t}{30}(2\mathbf{f}_1+16\mathbf{f}_2+2\mathbf{f}_3) \\ \frac{\Delta t}{30}(-\mathbf{f}_1+2\mathbf{f}_2+4\mathbf{f}_3) \end{Bmatrix} \tag{12}$$

Obviously, solving Eq. 12 is relatively difficult because this equation is coupled and six times larger than the original Eq. 1. Designing an iterative predictor/multi-corrector algorithm decreases the computational cost. Herein, rearranging the first, second and third equations in Eq. 12, the variables $\boldsymbol{v}_3$, $\boldsymbol{u}_2$ and $\boldsymbol{u}_3$ are represented as follows:

$$\begin{aligned} \mathbf{v}_3 &= \frac{15}{2}\overline{\mathbf{u}}_1^- - \frac{15}{2}\overline{\mathbf{u}}_1 - \mathbf{v}_1 + 2\mathbf{v}_2 \\ \mathbf{u}_2 &= \frac{15}{8}\mathbf{u}_1^- - \frac{7}{8}\mathbf{u}_1 + \frac{1}{4}\Delta t\mathbf{v}_1 + \frac{1}{4}\Delta t\mathbf{v}_2 \\ \mathbf{u}_3 &= -\frac{3}{2}\mathbf{u}_1^- + \frac{5}{2}\mathbf{u}_1 + \Delta t\mathbf{v} \end{aligned} \tag{13}$$

where, let $\overline{\mathbf{u}}_1 = 2\mathbf{u}_1/\Delta t$ and $\overline{\mathbf{u}}_1^- = 2\mathbf{u}_1^-/\Delta t$.

In order to obtain a better behavior of stability [Chien and Wu (2000)] for the iterative solution techniques, the system Eq. 12 is reduced to the following system equation:

$$\begin{bmatrix} \frac{2}{3}\mathbf{M}+\frac{1}{6}\Delta t\mathbf{C}+\frac{1}{60}\Delta t^2\mathbf{K} & \frac{1}{3}\mathbf{M}-\frac{1}{60}\Delta t^2\mathbf{K} & -\frac{5}{4}\mathbf{M}-\frac{1}{4}\Delta t\mathbf{C}-\frac{1}{240}\Delta t^2\mathbf{K} \\ -\frac{11}{6}\mathbf{M}-\frac{1}{4}\Delta t\mathbf{C}+\frac{19}{120}\Delta t^2\mathbf{K} & \frac{11}{6}\mathbf{M}+\frac{7}{6}\Delta t\mathbf{C}+\frac{17}{40}\Delta t^2\mathbf{K} & \frac{85}{8}\mathbf{M}+2\Delta t\mathbf{C}+\frac{31}{480}\Delta t^2\mathbf{K} \\ -\frac{1}{3}\mathbf{M}-\frac{1}{6}\Delta t\mathbf{C}+\frac{1}{60}\Delta t^2\mathbf{K} & \frac{1}{3}\mathbf{M}+\frac{1}{3}\Delta t\mathbf{C}+\frac{3}{20}\Delta t^2\mathbf{K} & \frac{15}{4}\mathbf{M}+\Delta t\mathbf{C}+\frac{29}{240}\Delta t^2\mathbf{K} \end{bmatrix} \begin{Bmatrix} \mathbf{v}_1 \\ \mathbf{v}_2 \\ \overline{\mathbf{u}}_1 \end{Bmatrix} =$$
$$\begin{Bmatrix} \mathbf{F}_1 + \left(-\frac{5}{4}\mathbf{M}-\frac{1}{4}\Delta t\mathbf{C}-\frac{7}{80}\Delta t^2\mathbf{K}\right)\overline{\mathbf{u}}_1^- + \mathbf{M}\mathbf{v}_1^- \\ \mathbf{F}_2 + \left(\frac{45}{8}\mathbf{M}+2\Delta t\mathbf{C}-\frac{63}{160}\Delta t^2\mathbf{K}\right)\overline{\mathbf{u}}_1^- \\ \mathbf{F}_3 + \left(\frac{15}{4}\mathbf{M}+\Delta t\mathbf{C}+\frac{3}{80}\Delta t^2\mathbf{K}\right)\overline{\mathbf{u}}_1^- \end{Bmatrix} \tag{14}$$

where
$\mathbf{F}_1 = \frac{\Delta t}{30}(4\mathbf{f}_1+2\mathbf{f}_2-\mathbf{f}_3)$, $\mathbf{F}_2 = \frac{\Delta t}{30}(2\mathbf{f}_1+16\mathbf{f}_2+2\mathbf{f}_3)$ and $\mathbf{F}_3 = \frac{\Delta t}{30}(-\mathbf{f}_1+2\mathbf{f}_2+4\mathbf{f}_3)$.

Clearly, the first, fourth and fifth equations in Eq. 12 have been partially decoupled from the second, third and sixth and, hence, Eq. 14 can be solved separately. Given initial predictor values of $\mathbf{v}_1$, $\mathbf{v}_2$ and $\overline{\mathbf{u}}_1$, for instance, the chosen values being $\mathbf{v}_1^-$ and $\overline{\mathbf{u}}_1^-$, Eq. 14 is solved iteratively for the corrected values of $\mathbf{v}_1$, $\mathbf{v}_2$ and $\overline{\mathbf{u}}_1$, respectively, until an accuracy requirement of $\varepsilon = 10^{-6}$ is obtained. Then, Eq. 13 is used for determining $\mathbf{u}_2$, $\mathbf{u}_3$ and $\mathbf{v}_2$. The above solution algorithm is summarized in Tab. 1. Notably, this table adopts the accelerated Gauss-Seidel method with the acceleration parameter α(i.e., the value 1.05 used in this study), which is known as the successive over-relaxation (or SOR) method. The SOR method can be used to accelerate the convergence when solving the linear system of equations. In each example of this study, the number of iterations using Gauss-Seidel algorithm per time step is only $4 \sim 7$ times. This procedure is superior to that described in the paper by Li and Wiberg (1996) (Using Gauss-Jacobi iteration method) [Chien and Wu (2000)]. It should be noted that the effective mass matrix $\mathbf{M}_2^*$ and generalized force vectors $\mathbf{F}_2^*$ are modified to achieve the stability with better behavior in the computation of iterative procedures.

Table 1: Implementation of the P2-P2 TDG method

A. Data input and initialization

$$\overline{\mathbf{u}}_1 = 2\mathbf{u}_0/\Delta t \ ; \ \mathbf{v}_1^- = \mathbf{v}_0 \ ; \ t = 0$$

B. Form effective mass matrix and perform factorization

$$\begin{aligned} \mathbf{M}_1^\star &= \tfrac{2}{3}\mathbf{M}+\tfrac{1}{6}\Delta t\mathbf{C}+\tfrac{1}{60}\Delta t^2\mathbf{K} \\ \mathbf{M}_2^\star &= \tfrac{11}{6}\mathbf{M}+\tfrac{7}{6}\Delta t\mathbf{C}+\tfrac{17}{40}\Delta t^2\mathbf{K} \\ \mathbf{M}_3^\star &= \tfrac{15}{4}\mathbf{M}+\Delta t\mathbf{C}+\tfrac{29}{240}\Delta t^2\mathbf{K} \end{aligned}$$

C. Time integration

(a) Form generalized force vectors

$$\begin{aligned} \mathbf{F}_1^\star &= \mathbf{F}_1 = \left(-\tfrac{5}{4}\mathbf{M}-\tfrac{1}{4}\Delta t\mathbf{C}-\tfrac{7}{80}\Delta t^2\mathbf{K}\right)\overline{\mathbf{u}}_1^- + \mathbf{M}\mathbf{v}_1^- \\ \mathbf{F}_2^\star &= \mathbf{F}_2 = \left(\tfrac{45}{8}\mathbf{M}+2\Delta t\mathbf{C}-\tfrac{63}{160}\Delta t^2\mathbf{K}\right)\overline{\mathbf{u}}_1^- \\ \mathbf{F}_3^\star &= \mathbf{F}_3 = \left(\tfrac{15}{4}\mathbf{M}+\Delta t\mathbf{C}-\tfrac{3}{80}\Delta t^2\mathbf{K}\right)\overline{\mathbf{u}}_1^- \end{aligned}$$

(b) Predictor phase

$$\mathbf{v}_1 = \mathbf{v}_1^- \ ; \ \mathbf{v}_2 = \mathbf{v}_1^- \ ; \ \overline{\mathbf{u}}_1 = \overline{\mathbf{u}}_1^- \ ; \ i = 0$$

(c) Multi-corrector phase (using SOR block interation)

$$\mathbf{M}_1^\star \mathbf{v}_1^{(i+1)} = \mathbf{F}_1^\star - \left(\tfrac{1}{3}\mathbf{M}-\tfrac{1}{60}\Delta t^2\mathbf{K}\right)\mathbf{v}_2^{(i)} + \left(\tfrac{5}{4}\mathbf{M}+\tfrac{1}{4}\Delta t\mathbf{C}+\tfrac{1}{240}\Delta t^2\mathbf{K}\right)\overline{\mathbf{u}}_1^{(i)}$$

$\mathbf{v}_1^{(i+1)} = \alpha\mathbf{v}_1^{(i+1)} + (1-\alpha)\mathbf{v}_1^{(i)}$

$\mathbf{M}_3^{\star}\overline{\mathbf{u}}_1^{(i+1)} = \mathbf{F}_3^{\star} - \left(-\frac{1}{3}\mathbf{M} - \frac{1}{6}\Delta t\mathbf{C} + \frac{1}{60}\Delta t^2\mathbf{K}\right)\mathbf{v}_1^{(i+1)} - \left(\frac{1}{3}\mathbf{M} + \frac{1}{3}\Delta t\mathbf{C} + \frac{3}{20}\Delta t^2\mathbf{K}\right)\mathbf{v}_2^{(i+1)}$

$\overline{\mathbf{u}}_1^{(i+1)} = \alpha\overline{\mathbf{u}}_1^{(i+1)} + (1-\alpha)\overline{\mathbf{u}}_1^{(i)}$

$\mathbf{M}_2^{\star}\mathbf{v}_2^{(i+1)} = \mathbf{F}_2^{\star} - \left(-\frac{11}{6}\mathbf{M} - \frac{1}{4}\Delta t\mathbf{C} + \frac{19}{120}\Delta t^2\mathbf{K}\right)\mathbf{v}_1^{(i+1)} - \left(\frac{85}{8}\mathbf{M} + 2\Delta t\mathbf{C} + \frac{31}{480}\Delta t^2\mathbf{K}\right)\overline{\mathbf{u}}_1^{(i)}$

$\overline{\mathbf{v}}_2^{(i+1)} = \alpha\overline{\mathbf{v}}_2^{(i+1)} + (1-\alpha)\overline{\mathbf{v}}_2^{(i)}$

If $||\mathbf{v}_1^{i+1} - \mathbf{v}_1^i, \mathbf{v}_2^{i+1} - \mathbf{v}_2^i, \overline{\mathbf{u}}_1^{i+1} - \overline{\mathbf{u}}_1^i|| \le \varepsilon$

If $\overline{\varepsilon} > \varepsilon$ got to (c), else $i = i+1$

(d) Output solution

$\mathbf{v}_3 = \frac{15}{2}\overline{\mathbf{u}}_1^- - \frac{15}{2}\overline{\mathbf{u}}_1 - \mathbf{v}_1 + 2\mathbf{v}_2$

$\mathbf{u}_2 = \frac{15}{8}\mathbf{u}_1^- - \frac{7}{8}\mathbf{u}_1 + \frac{1}{4}\Delta t\mathbf{v}_1 + \frac{1}{4}\Delta t\mathbf{v}_2$

$\mathbf{u}_3 = -\frac{3}{2}\mathbf{u}_1^- + \frac{5}{2}\mathbf{u}_1 + \Delta t\mathbf{v}_2$

$\mathbf{v}_1^- \leftarrow \mathbf{v}_3$

$\overline{\mathbf{u}}_1^- \leftarrow \mathbf{u}_3$.

If $t < T$ go to (a), else terminate

4 Stability and Accuracy

This section adopts the spectral approach to examine the stability and accuracy of the TDG solution algorithm using the P2-P2 element for the second-order ordinary differential equations in the time domain [Hughes (1987); Bathe (1996)]. Also, the P1-P1 TDG method as well as the well-known direct time integration methods are discussed in terms of their corresponding parameters with better accuracy. In addition, two measures are used to discuss the accuracy analysis: algorithmic damping ratio and relative period error. Stability and accuracy should be taken into account when considering the effectiveness of an iterative solution method [Hughes (1987); Bathe (1996)].

4.1 Stability Analysis

In stability analysis, it is convenient to work with the undamped, free vibration single degree-of-freedom model problem:

$$\ddot{u} + \omega u = 0 \tag{15}$$

where ω denotes the undamped angular frequency. Although this equation is not the same as the original multi-DOF system Eq. 1, its stability implies the stability of the corresponding original multi-DOF system equation. Thus, Eq. 12 can be reduced to the simple form:

$$\begin{bmatrix} \frac{1}{2}\omega^2 & \frac{2}{3}\omega^2 & -\frac{1}{6}\omega^2 & -\frac{2}{15}\Delta t\omega^2 \\ -\frac{2}{3}\omega^2 & 0 & \frac{2}{3}\omega^2 & -\frac{1}{15}\Delta t\omega^2 \\ \frac{1}{6}\omega^2 & -\frac{2}{3}\omega^2 & \frac{1}{2}\omega^2 & \frac{1}{30}\Delta t\omega^2 \\ \frac{2}{15}\Delta t\omega^2 & \frac{1}{15}\Delta t\omega^2 & -\frac{1}{30}\Delta t\omega^2 & \frac{1}{2} \\ \frac{1}{15}\Delta t\omega^2 & \frac{8}{15}\Delta t\omega^2 & \frac{1}{15}\Delta t\omega^2 & -\frac{2}{3} \\ -\frac{1}{30}\Delta t\omega^2 & \frac{1}{15}\Delta t\omega^2 & \frac{2}{15}\Delta t\omega^2 & \frac{1}{6} \end{bmatrix} \begin{bmatrix} -\frac{1}{15}\Delta t\omega^2 & \frac{1}{30}\Delta t\omega^2 \\ -\frac{8}{15}\Delta t\omega^2 & -\frac{1}{15}\Delta t\omega^2 \\ -\frac{1}{15}\Delta t\omega^2 & -\frac{2}{15}\Delta t\omega^2 \\ \frac{2}{3} & -\frac{1}{6} \\ 0 & \frac{2}{3} \\ -\frac{2}{3} & \frac{1}{2} \end{bmatrix} \begin{Bmatrix} u_1 \\ u_2 \\ u_3 \\ v_1 \\ v_2 \\ v_3 \end{Bmatrix} = \begin{Bmatrix} \omega^2 u_1^- \\ 0 \\ 0 \\ v_1^- \\ 0 \\ 0 \end{Bmatrix} \tag{16}$$

Herein, v_3 and u_3 can be determined in terms of u_1^- and v_1^- and then rearranged in a matrix form, as follows:

$$\begin{Bmatrix} v_3 \\ u_3 \end{Bmatrix} = [\mathbf{A}] \begin{Bmatrix} v_1^- \\ u_1^- \end{Bmatrix} \tag{17}$$

in which the matrix $[\mathbf{A}]$ denotes the amplification matrix. The explicit form is given as follows:

$$[A] = \frac{1}{H}\begin{bmatrix} 3600 - 1584\,(\omega\Delta t)^2 + 51\,(\omega\Delta t)^4 & \\ \Delta t\left[3600 - 384\,(\omega\Delta t)^2 + 3\,(\omega\Delta t)^4\right] & \\ \frac{1}{\Delta t}\left[-3600\,(\omega\Delta t)^2 + 384\,(\omega\Delta t)^4 - 3\,(\omega\Delta t)^6\right] & 3600 - 1584\,(\omega\Delta t)^2 + 51\,(\omega\Delta t)^4 \end{bmatrix} \tag{18}$$

where $H = 3600 + 216\,(\omega\Delta t)^2 + 9\,(\omega\Delta t)^4 + (\omega\Delta t)^6$. The method is stable if each spectral radius satisfies the following condition [Hughes (1987); Bathe (1996)], i.e.,

$$\rho\left([A]\right) \le 1 \tag{19}$$

where the spectral radius ρ is defined as

$$\rho\left([A]\right) = \max\left|\lambda_i\right|,\ i = 1,2 \tag{20}$$

and $\lambda_i([\boldsymbol{A}])$ denotes the ith eigenvalues of amplification matrix $[\boldsymbol{A}]$. Since $\rho([\boldsymbol{A}])$ satisfies Eq. 19 for the stability condition, the recurrence Eq. 17 is unconditionally stable. The spectral radii of the amplification matrix are plotted in Fig. 3 for the P2-P2 TDG method as well as for the P1-P1 TDG and commonly used direct time

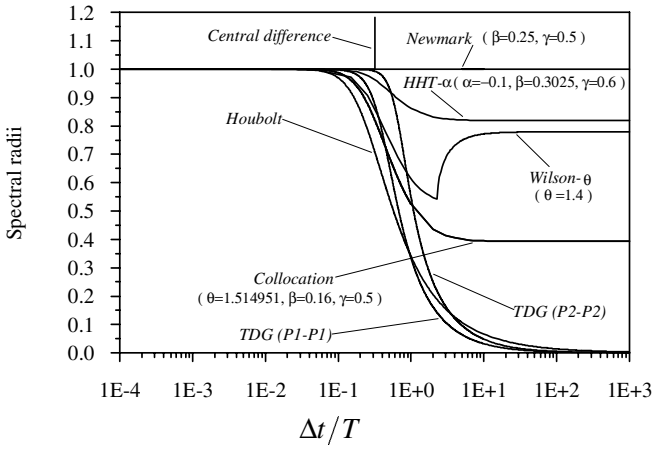

Figure 3 : Comparison of spectral radii for TDG (P2-P2), TDG (P1-P1), Central difference, Collocation, Houbolt, Wilson-θ, HHT-α and Newmark methods

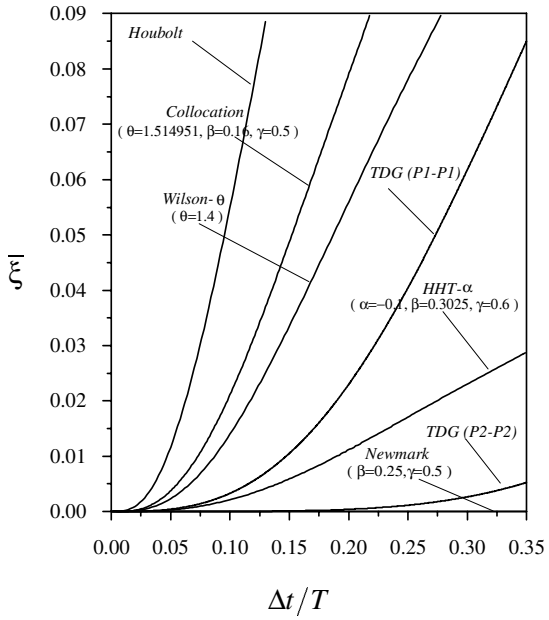

Figure 4 : Comparison of algorithmic damping ratios for TDG (P2-P2), TDG (P1-P1), Collocation, Houbolt, Wilson-θ, HHT-α and Newmark methods.

integration methods [Hulbert (1994); Bathe (1996)]. In Fig. 3, the method called "Newmark ($\beta = 0.25, \gamma = 0.5$)" corresponds to the average - acceleration method (also called trapezoidal rule) [Bathe (1996)]. The P2-P2 TDG method refers to the present method which behaves better than other methods. Herein, the P2-P2 method succeeds in asymptotically annihilating spurious high-frequency behavior without introducing excessive dissipation in the low-frequency regime.

4.2 Accuracy Analysis

Accuracy refers to the difference between the numerical solution and the exact solution when the numerical solution process is stable.

If the eigenvalues of [$\boldsymbol{A}$] remain complex, ie.,

$$\lambda_{1,2} = A \pm Bi = e^{\left(-\overline{\xi} \pm i\right)\overline{\Omega}} = e^{-\overline{\xi}\overline{\Omega}} \left(cos\overline{\Omega} \pm isin\overline{\Omega}\right) \tag{21}$$

in which $i = \sqrt{-1}$ and $B \neq 0$,and define $\Omega = \omega\Delta t$ and $\overline{\Omega} = \overline{\omega}\Delta t$ ($\overline{\omega}$ is the approximate frequency evaluated from a numerical solution).

From Eq. 21, we can obtain the following expression:

$$\overline{\Omega} = \tan^{-1}\left(B/A\right) \tag{22}$$

$$\overline{\xi} = \frac{-\ln\left(A^2 + B^2\right)}{2\overline{\Omega}} \tag{23}$$

where $\overline{\xi}$ is the algorithmic damping ratio. The algorithmic damping ratio provides a measure of the numerical dissipation.

The relative period error is taken as the measure of numerical dispersion and is calculated using

$$\frac{\overline{T} - T}{T} = \frac{\omega}{\overline{\omega}} - 1 = \frac{\Omega}{\overline{\Omega}} - 1 = \frac{2\pi\left(\Delta t/T\right)}{\tan^{-1}\left(B/A\right)} \tag{24}$$

where $T = 2\pi/\omega$ and $\overline{T} = 2\pi/\overline{\omega}$ are the exact natural period and the approximate natural period evaluated from a numerical solution, respectively.

The algorithmic damping ratios and the relative period errors are plotted and compared with other known methods in Figs. 4 and 5, respectively. Fig. 4 reveals that the P2-P2 algorithm has very little numerical dissipation in the low-frequency regime. Meanwhile, Fig. 5 indicates that the period error of the P2-P2 algorithm is virtually negligible in the low-frequency regime, which reflects its fifth-order accuracy. Fig. 5 makes the third-order accuracy of the P1-P1 method evident. Meanwhile, commonly used direct time integration methods are only second-order accurate [Hulbert (1994)].

Above discussion confirms that the TDG method using P2-P2 elements is an effective, stable and accurate algorithm.

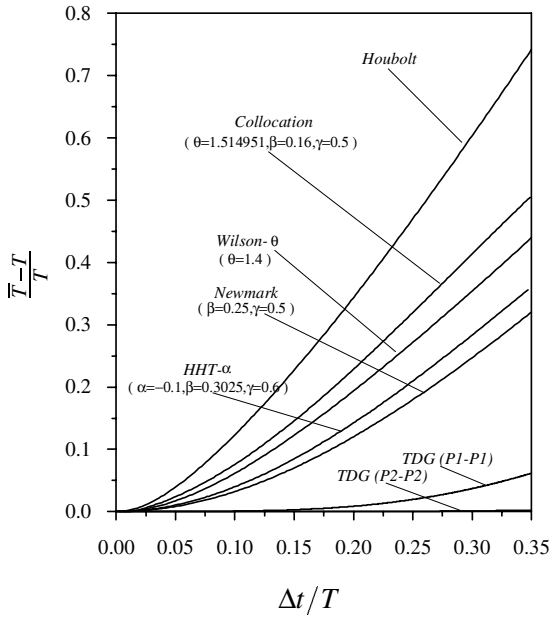

Figure 5 : Comparison of relative period errors for TDG (P2-P2), TDG (P1-P1), Collocation, Houbolt, Wilson-θ, HHT-α and Newmark methods.

5 Numerical examples

Commonly used direct time integration methods produce less accurate solutions than the TDG method for second-order ordinary differential equations in the time domain. Hence, numerical results presented herein only use the P1-P1 and P2-P2 TDG methods. The efficiency and accuracy of this approach is demonstrated by using the P2-P2 element for several benchmark problems in structural dynamics application [Li and Wiberg (1996); Bathe (1996)].

Example 1: SDOF model

The equation of motion for the SDOF model has the form

$$\begin{aligned} &m\ddot{u}+c\dot{u}+ku=f(t) \\ &u(0)=u_0, \qquad \dot{u}(0)=v_0 \end{aligned} \tag{25}$$

Example 1a: Assume that m = 1, c = 0, k = 1, $f(t)$ = 0 and u_0 = 1, v_0 = 0. This is the example of an undamped free vibration. A time step Δt = 0.1 is used for the computation. Fig. 6 plots the responses and the error distributions.

Example 1b: Assume that m = 1, c = 0.1, k = 1, $f(t)$ = sin0.5t and u_0 = 0, v_0 = 0. This is the example of a damped forced vibration. A time step Δt = 0.1 is also used for the computation. Fig. 7 plots the responses and the error distributions.

Figs. 6 and 7 compare with the P1-P1 element solution and the exact solution, revealing that the P2-P2 method provides a much more accurate solution than the P1-P1 method. Figs. 8 and 9 show the convergence of numerical solutions at time t = 10.0 sec, for *Example 1a* and *1b*, respectively. The graphs indicate that, while the P1-P1 TDG method is only third-order accurate, the proposed approach using the P2-P2 element is of fifth-order accuracy.

Example 2: Two-DOF model

Fig. 10 illustrates a two-DOF system for which the governing equations are

$$\begin{bmatrix} m_1 & 0 \\ 0 & m_2 \end{bmatrix} \begin{Bmatrix} \ddot{u}_1 \\ \ddot{u}_2 \end{Bmatrix} + \begin{bmatrix} k_1+k_2 & -k_2 \\ -k_2 & k_2+k_3 \end{bmatrix} \times \begin{Bmatrix} u_1 \\ u_2 \end{Bmatrix} = \begin{Bmatrix} f_1 \\ f_2 \end{Bmatrix} \tag{26}$$

In the following examples we consider two different cases.

Example 2a: Assume that $m_1 = 2, m_2 = 1, k_1 = 4, k_2 = 2, k_3 = 2, f_1 = 1, f_2 = 10$ and zero initial conditions. A fixed time step size $\Delta t = T_2/10$, where $T_2 = 2.8$ is the lower period of the system, is used by the P2-P2 method for the calculation. Numerical results are also obtained by the P1-P1 TDG method, and with the application of the same step size. Figs. 11 and 12 depict the responses and error distributions of the displacements and the velocities, respectively. The results observed are similar to *Example 1*. The proposed method more closely corresponds to the exact solution than that of the P1-P1 method.

Example 2b: Assume that $m_1 = 1, m_2 = 1, k_1 = 10^4, k_2 = 1, k_3 = 0, f_1 = 0, f_2 = 0$ and $u_1(0) = 1, u_2(0) = 10, v_1(0) = 0, v_2(0) = 0$. This example is used to represent the character of typical large systems by Hughes (1987). The first mode represents those modes that are physically important and must be accurately evaluated. The second mode represents those spurious high modes whose filtering by numerical time integration is desirable. We use a fixed time step size Δt = 0.314 (i.e. T_1/20,where T_1 is the higher period of the system) to perform the time integration. The numerical solutions obtained by both the P1-P1 and P2-P2 TDG finite element method are presented in Fig. 13. Fig. 13 reveals that the

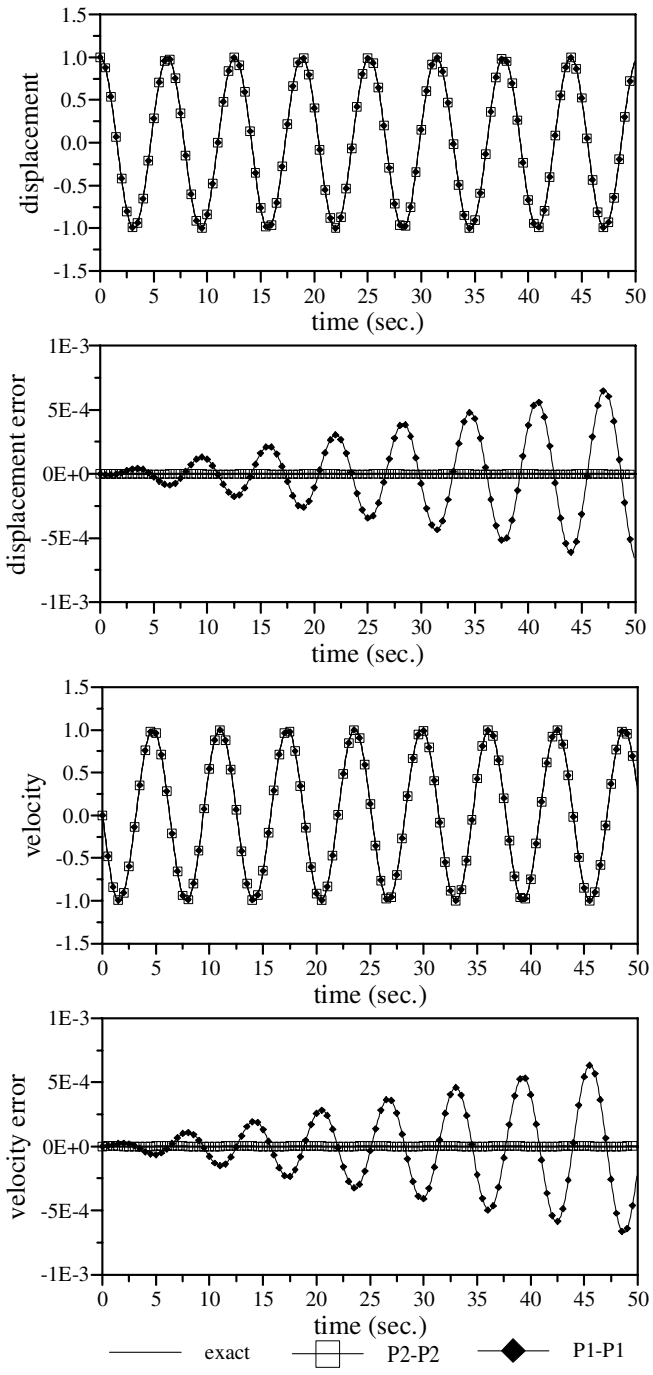

Figure 6 : Responses and error distributions for the SDOF system under undamped free vibration with Δt = 0.1 sec (*Example 1a*)

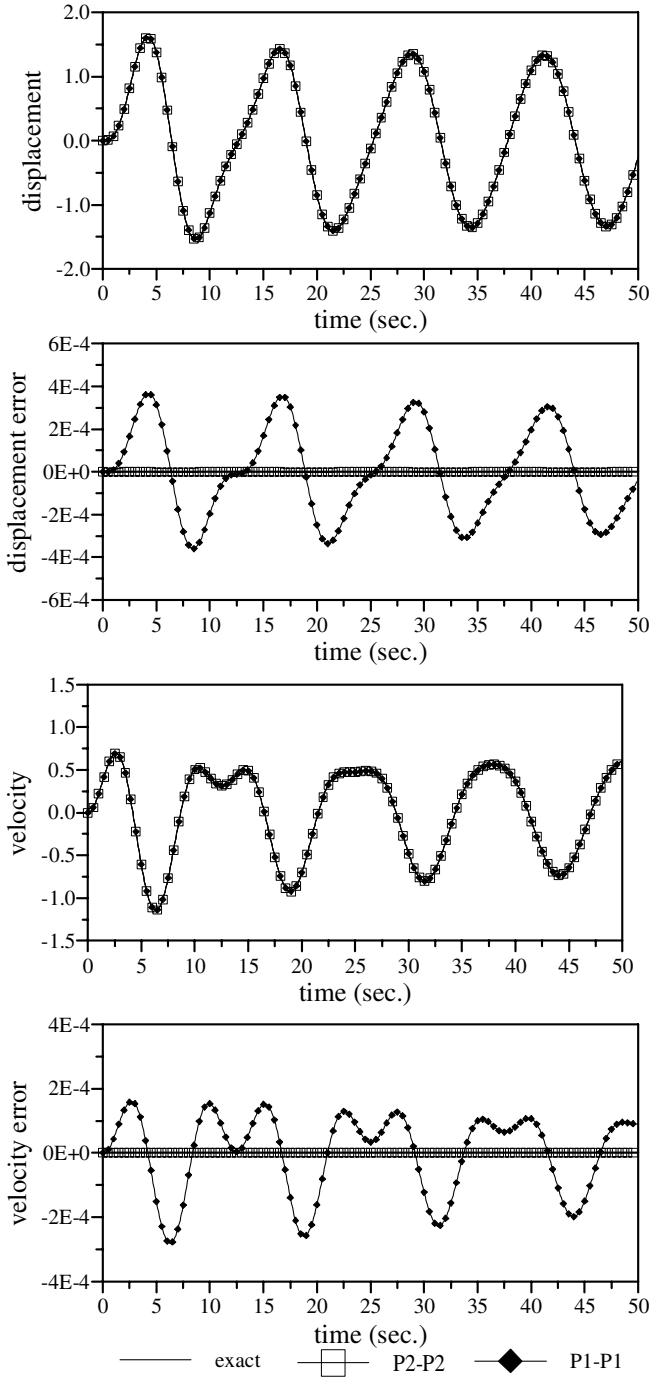

Figure 7 : Responses and error distributions for the SDOF system under damped forced vibration with Δt = 0.1 sec (*Example 1b*)

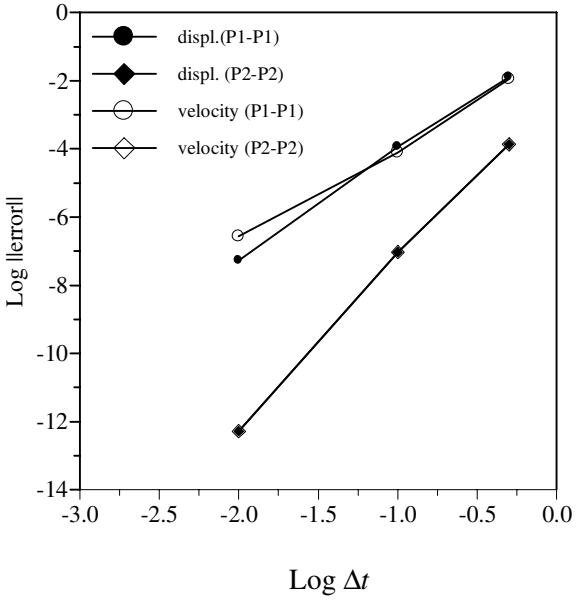

Figure 8 : Rate of convergence at time t = 10.0 sec for displacement and velocity (*Example 1a*)

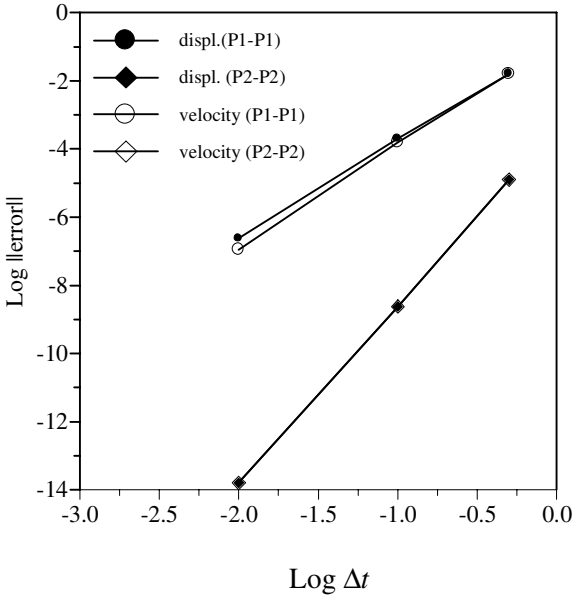

Figure 9 : Rate of convergence at time t = 10.0 sec for displacement and velocity (*Example 1b*)

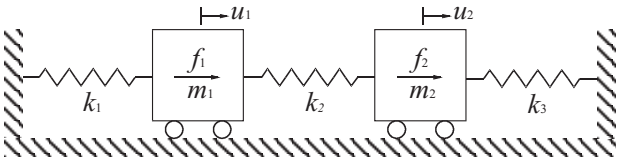

Figure 10 : A two - DOF system

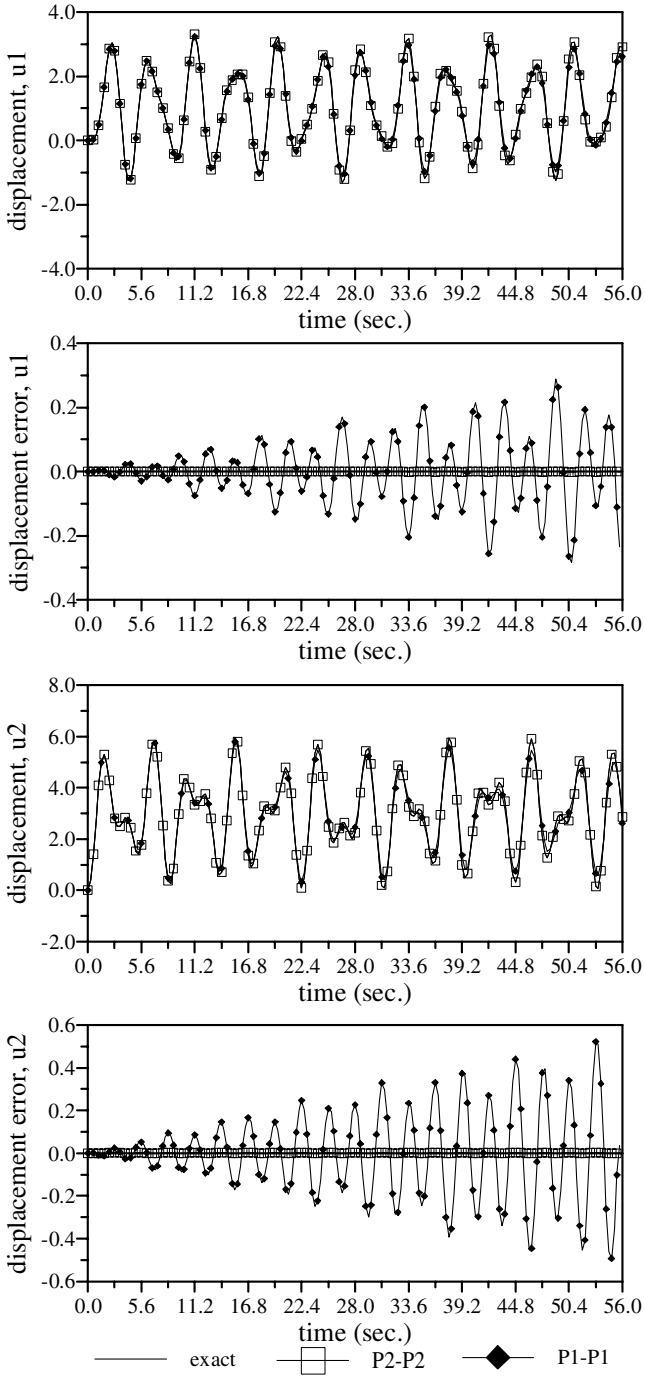

Figure 11 : Displacement responses and error distributions for the two-DOF system ith Δt = 0.28 sec (*Example 2a*)

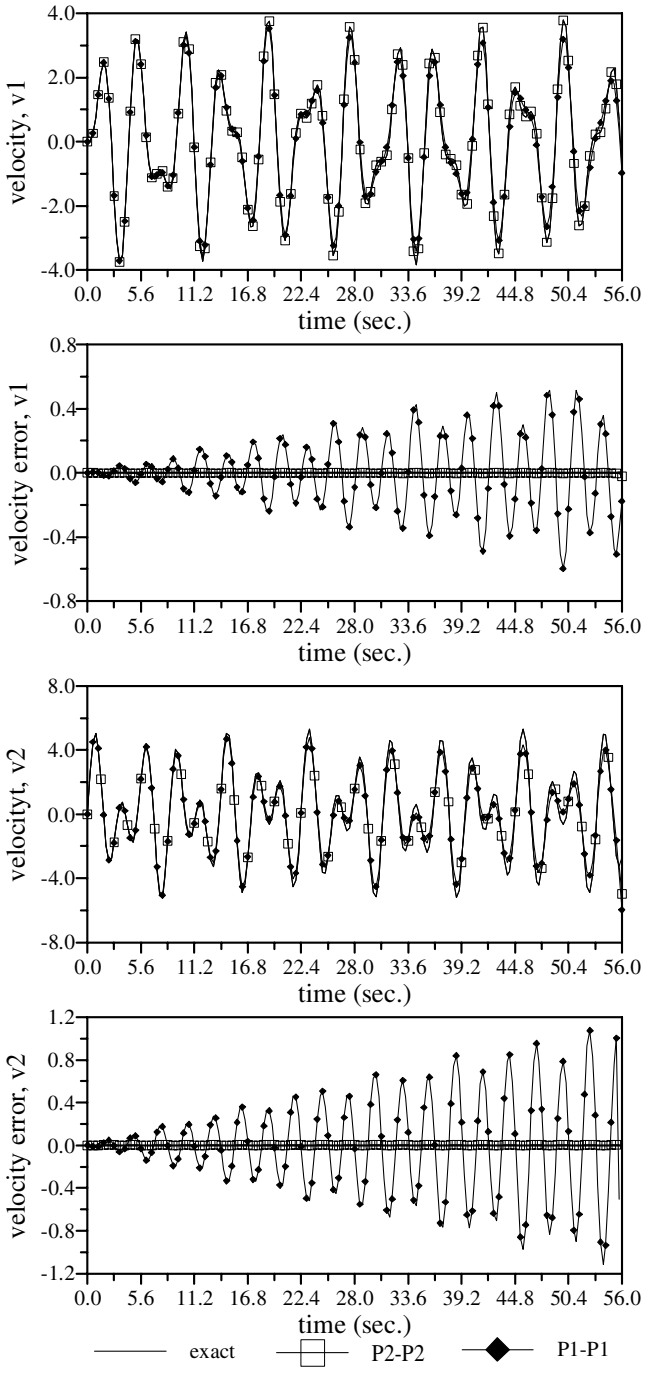

Figure 12 : Velocity responses and error distributions for the two-DOF system with Δt = 0.28 sec (*Example 2a*)

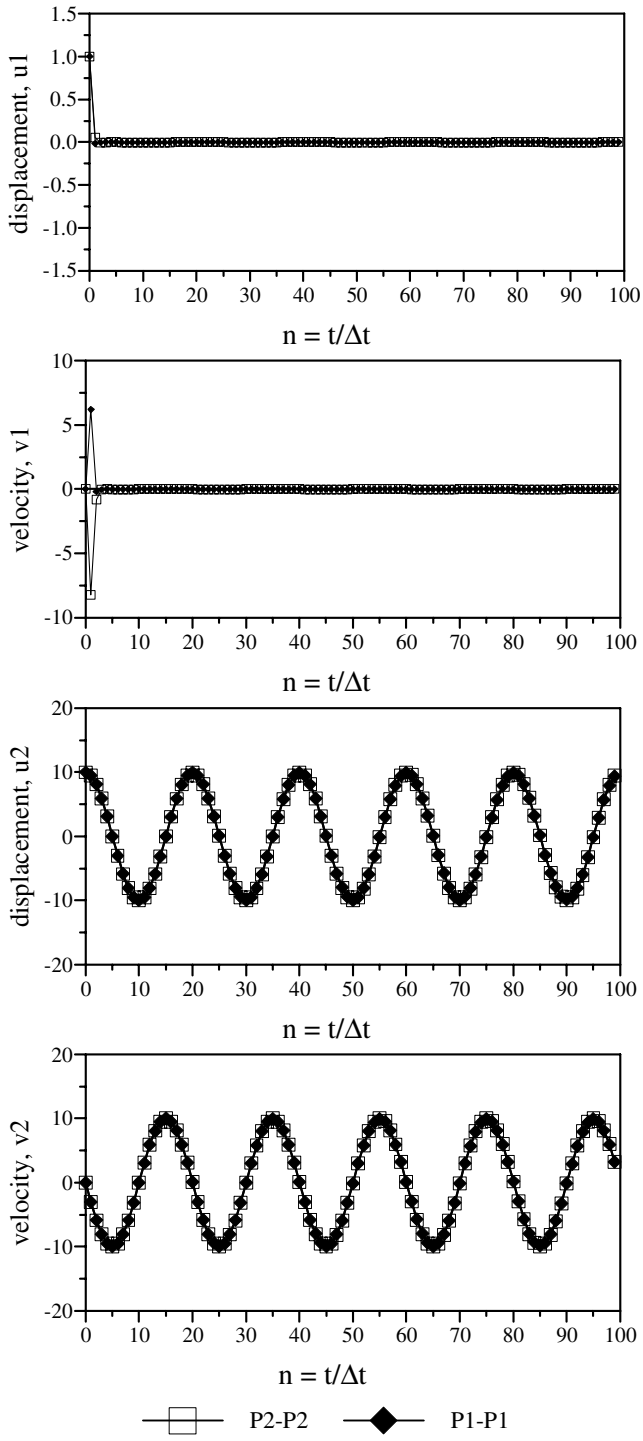

Figure 13 : Responses of the two-DOF system with Δt = T_1 / 20 sec (*Example 2b*)

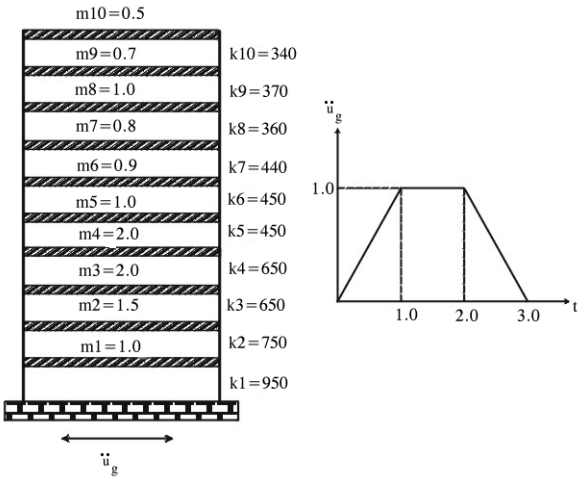

Figure 14 : A ten-story shear building subjected to a base-acceleration pulse

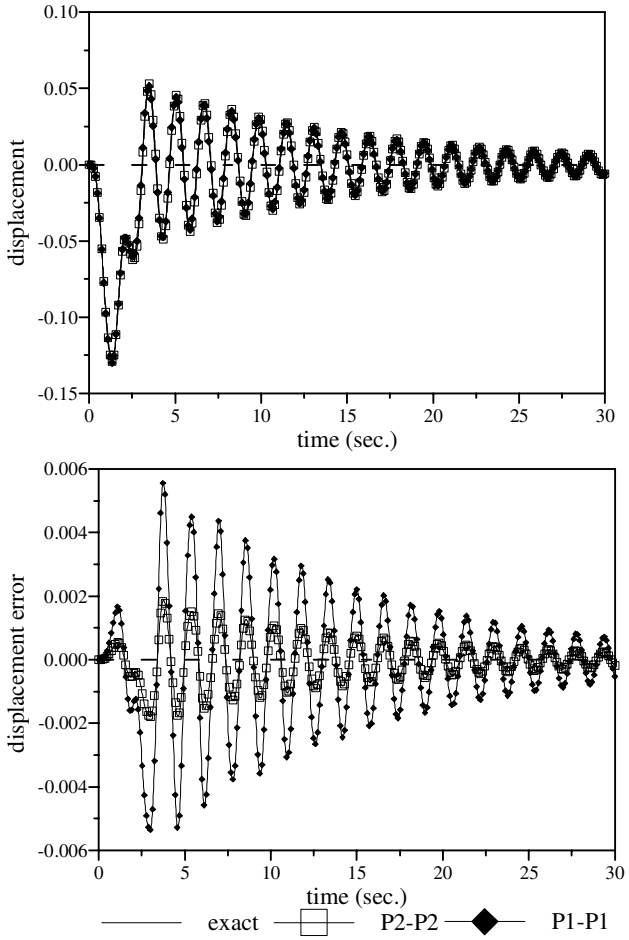

Figure 15 : Displacement response histories and error distributions of the ten-story shear building at the top with Δt = 0.02 sec

TDG method provides very good results in the sense that the important mode has been accurately integrated and the spurious one successfully filtered. Other commonly used integration schemes, such as the Newmark method, were performed on this model which produced less accurate solution without filtering out the high frequency modes [Li and Wiberg (1996); Hughes (1987)].

Example 3: A shear building subjected to a base-acceleration pulse

As a multi-DOF system, this example involves a ten-story shear building, the base of which is subjected to a base-acceleration pulse, as shown in Fig. 14. The data on mass and stiffness are taken from Li and Wiberg (1996) and Torkamani and Ahmadi (1988). Rayleigh damping is assumed and the parameters are selected to be 2%. Two time steps Δt = 0.02 sec and Δt = 0.05 sec are used for the computation, respectively. The P1-P1 and P2-P2 TDG methods are used to perform an analysis over a time interval [0, 30 sec]. Histories for displacement and velocity including error distributions at the top and shear force including error distributions at the bottom are plotted in Figs. 15∼17, respectively, with the time step Δt = 0.02 sec, and in Figs. 18∼20 with Δt = 0.05 sec. The graphs display that the P2-P2 method still performs better than the P1-P1 method does. Specifically, the P1-P1 method introduces more amplitude decay and period elongation than the P2-P2 method. Notably, even for the stiff structure, a very accurate solution can be obtained by the TDG method with a fairly big step size, a result which the Newmark method cannot achieve [Li and Wiberg (1996)].

6 Conclusions

This work has presented an advanced time finite element formulation which is implemented for the structural dynamic problems. This formulation is based on the time-discontinuous Galerkin method in which both the unknown displacements and unknown velocities are approximated as piecewise three-noded quadratic interpolation functions in the time domain. This investigation has established the stability and accuracy of the P1-P1 and P2-P2 TDG methods as well as various traditionally used direct time integration algorithms. Numerical results from analyses of the P2-P2 TDG algorithm were

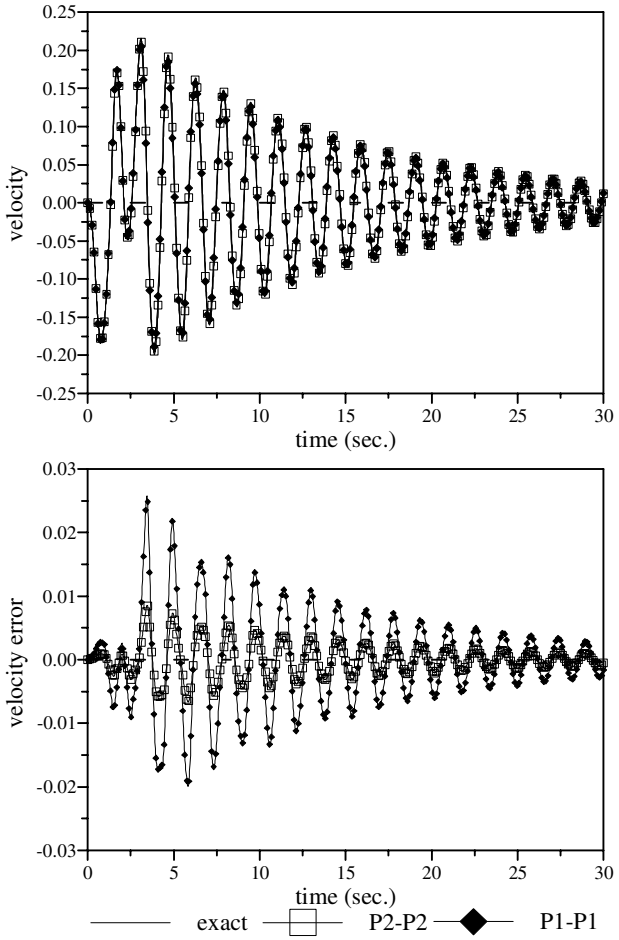

Figure 16 : Velocity response histories and error distributions of the ten-story shear building at the top with Δt = 0.02 sec

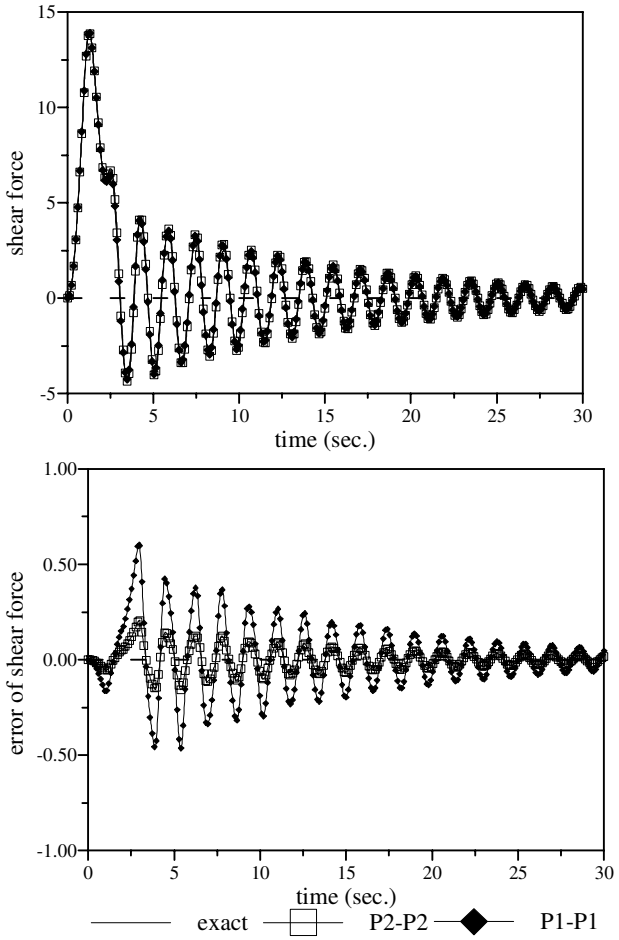

Figure 17 : Shear force response histories and error distributions of the ten-story shear building at the bottom with Δt = 0.02 sec

compared with the P1-P1 TDG method that has appeared in literature. The results demonstrate that the P2-P2 TDG method possesses advantages over the P1-P1 method and commonly used structural dynamics algorithms. In particular, the P2-P2 TDG algorithm achieves fifth order accuracy and the asymptotic annihilation property with a nearly optimal balance of computational expense and accuracy. However, the time-discontinuous Galerkin methods typically lead to systems of coupled equations that are larger than those emanating from standard semi-discrete methods. Therefore, enhanced predictor/multi-corrector algorithms must be developed to make the computation more efficient. However, even the proposed method can be extended to two- and three-dimensional elastodynamic problems.

References

Argyris, J.; Scharpf, D. W. (1969): Finite elements in time and space. *Nucl. Eng. Design,* vol. 10, pp. 456-464.

Borri, M.; Mello, F. J.; Atluri, S. N. (1990): Variational approaches for dynamics and time-finite-elements: numerical studies. *Comp. Mech.*, vol. 7, pp. 49-76.

Borri, M.; Bottasso, C. (1993): A general framework for interpreting time finite element formulations. *Comp. Mech.*, vol. 13, pp. 133-142.

Bathe, K.-J. (1996): *Finite Element Procedures.* Prentice-Hall Inc., Englewood Cliffs, NJ.

Chien, C.-C.; Wu, T.-Y. (2000): An improved predictor/multi-corrector algorithm for a time-discontinuous Galerkin finite element method in

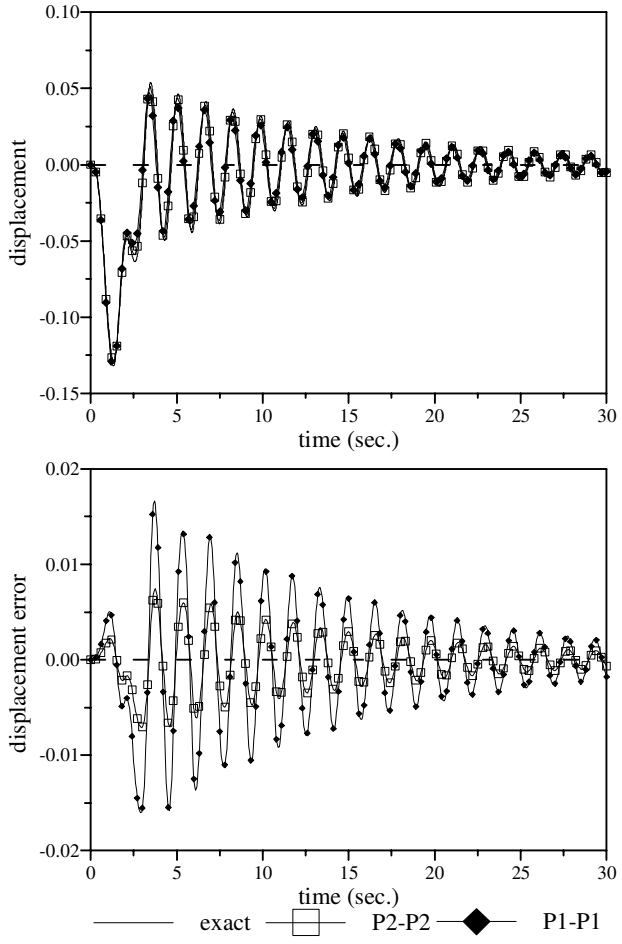

Figure 18 : Displacement response histories and error distributions of the ten-story shear building at the top with Δt = 0.05 sec

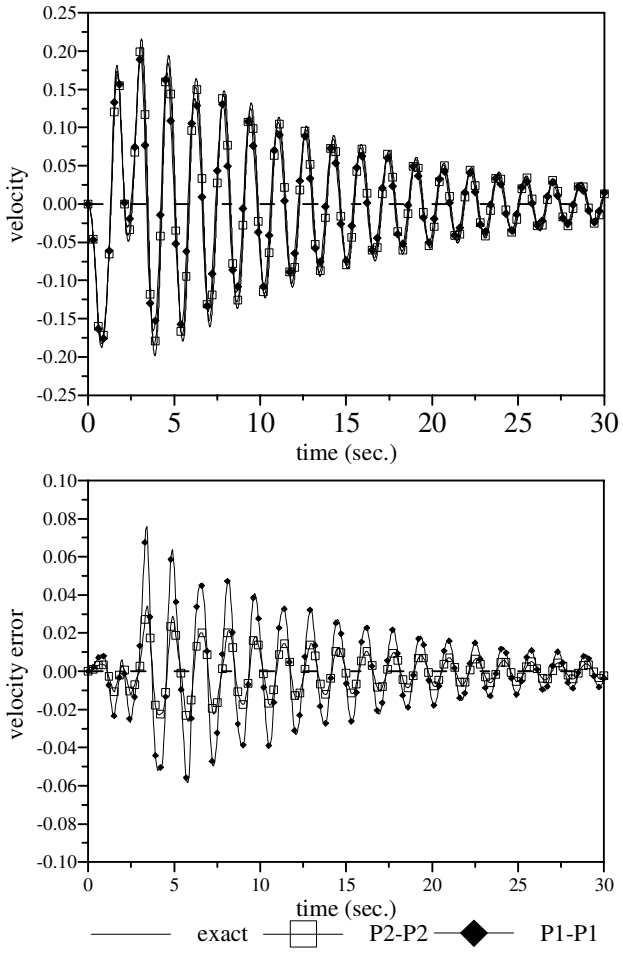

Figure 19 : Velocity response histories and error distributions of the ten-story shear building at the top with Δt = 0.05 sec

structural dynamics. *Comp. Mech.*, vol. 25, pp. 430-437.

Fried, I. (1969): Finite element analysis of time-dependent phenomena. *AIAA J.*, vol. 7, pp. 1170-1173.

Houbolt, J. C. (1950): A recurrence matrix solution for the dynamic response of elastic aircraft. *J. Aeronautical Sciences*, vol. 17, pp. 540-550.

Hilber, H. M.; Hughes, T. J. R.; Taylor, R. L. (1977): Improved numerical dissipation for time integration algorithms in structural dynamics. *Earthquake Eng. Struct. Dyn.*, vol. 5, pp. 283-292.

Hughes, T. J. R. (1987): *The Finite Element Method: Linear Static and Dynamic Finite Element Analysis*. Prentice-Hall Inc., Englewood Cliffs, NJ.

Hughes, T. J. R.; Hulbert, G. (1988): Space-time finite element methods for elastodynamics: Formulation and error estimates. *Comput. Methods Appl. Mech. Eng.,* vol. 66, pp. 393-363.

Hulbert, G.; Hughes, T. J. R. (1990): Space-time finite element methods for second order hyperbolic equations. *Comput. Methods Appl. Mech. Eng.,* vol. 84, pp. 327-348.

Hulbert, G. (1992): Time finite element methods for structural dynamics. *Int. J. Num. Methods Eng.,* vol. 33, pp. 307-331.

Hulbert, G. (1994): A unified set of single-step asymptotic annihilation algorithms for strcutural dynamics. *Comput. Methods Appl. Mech. Eng.*, vol. 113, pp.1-9.

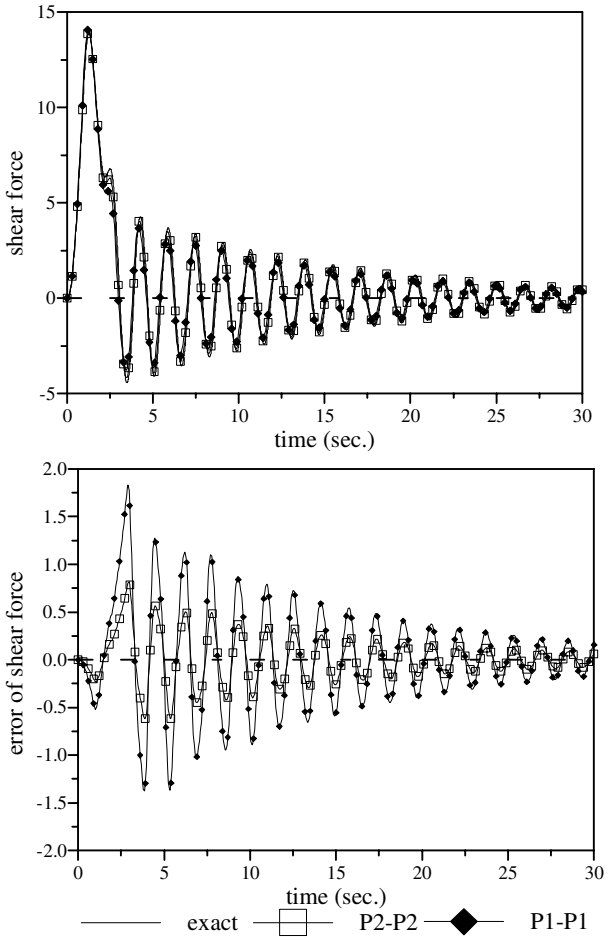

Figure 20 : Shear force response histories and error distributions of the ten-story shear building at the bottom with $\Delta t = 0.05$ sec

Johnson, C.; Nävert, U.; Pitkaranta, J. (1984): Finite element methods for linear hyperbolic problem. *Comput. Methods Appl. Mech. Eng.,* vol. 45, pp. 285-312.

Johnson, C. (1987): *Numerical Solutions of Partial Differential Equations by the Finite Element Method.* Cambridge Univ. Press, Cambridge.

Karaoğlan, L.; Noor, A. K. (1997): Space-time finite element methods for the sensitivity analysis of contact/impact response of axisymmetric composite structures. *Comput. Methods Appl. Mech. Eng.*, vol. 144, pp. 371-389.

Li, X. D.; Wiberg, N.-E. (1996): Structural dynamic analysis by a time-discontinuous Galerkin finite element method. *Int. J. Num. Methods Eng.,* vol. 39, pp. 2131-2152.

Li, X. D.; Wiberg, N.-E. (1998): Implementation and adaptivity of a space-time finite element method. *Comput. Methods Appl. Mech. Eng.,* vol. 156, pp. 211-229.

Mello, F. J.; Borri, M.; Atluri, S. N. (1990): Time finite element methods for large rotational dynamics of multibody systems. *Comput. Struct.*, vol. 37, pp. 231-240.

Newmark, N. M. (1959): A method of computation for structural dynamics. *ASCE J. Eng. Mech. Div.,* vol. 8, pp. 67-94.

Oden, J. T. (1969): A general theory of finite elements II, Applications. *Int. J. Num. Methods Eng.*, vol. 1, pp. 247-259.

Thomée, V. (1984): *Galerkin Finite Element Methods for Parabolic Problems.* Springer-Verlag, New York.

Torkamani, M. A. M.; Ahmadi, A. K. (1988): Stiffness identification of two- and three dimensional frames. *Earthquake Eng. Struct. Dyn.*, vol. 18, pp. 1157-1176.

Wilson, E. L.; Farhoomand, I.; Bathe, K.-J. (1973): Nonlinear dynamic analysis of complex structures. *Earthquake Eng. Struct. Dyn.,* vol. 1, pp. 242-252.

Zienkiewicz, O. C.; Taylor, R. L. (1991): *The Finite Element Method, vol. 2: Solid and Fluid Mechanics, Dynamics and Nonlinearity.* McGraw-Hill, Landon.

Acknowledgement: The authors would like to thank the National Science Council of the Republic of China for financially supporting this research under Contract No. NSC-88-2211-E-033-003.